Supporting Information

Simonetti et al. 10.1073/pnas.1522675113

SI Materials and Methods

The patient was a 58-y-old African-American man with an MSM risk factor and a 30-y history of smoking and alcohol use who was in good health until April 2000, when he developed thrush and was diagnosed with HIV-1 infection. Duration of the HIV-1 infection is uncertain; a prior HIV-1 ELISA performed in 1985 was negative. At diagnosis, he had 16 $CD4^+$ T cells/μL and viral RNA of 283,186 copies/mL plasma. He enrolled in an NIH study of antiretroviral therapy and viral decay kinetics (protocol 97-I-0027). On enrollment in an NIH natural history protocol of HIV infection in June of 2000, $CD4^+$ T-cell count was 22 cells/μL, his viral RNA level was 5.4 $\log_{10}$ copies/mL plasma, and therapy with azidothymidine, lamivudine, indinavir, and nevirapine was initiated.

The patient tolerated antiretroviral therapy, and viral RNA in the blood underwent typical initial first- and second-phase decay kinetics to <50 copies HIV RNA/mL within 4 mo; his $CD4^+$ T-cell count increased but never exceeded 350 cells/μL (Fig. S1). His course was marked by an episode of Kaposi sarcoma that developed within 6 mo of the initiation of cART. After 5 y of continuous therapy, he underwent several interruptions of cART due to insurance lapses. During these interruptions, he experienced rebound viremia, but there was prompt suppression of viremia when the therapy was restarted (Fig. S1*A*).

The patient remained well until December 2011, when he developed persistent low-level viremia (134 copies/mL) measured by bDNA, Versant 3.0. His $CD4^+$ T-cell count was stable at 153 cells/μL (12%). and he reported >95% adherence to cART. Commercial drug resistance testing (TRUGENE) revealed the presence of the following mutations in RT: L74V, M184V, K103N, and V108I; these mutations are known to confer some degree of resistance to all of the antiretroviral drugs in the regimen he was taking at that time (abacavir, lamivudine, and efavirenz).

At the time the persistent low-level viremia emerged, a physical examination identified several macerated papules on the dorsum of his tongue that were asymptomatic; shortly thereafter, the patient reported the presence of small mass on the dorsum of his tongue, which was subsequently diagnosed as stage III, T3N0 moderately differentiated squamous cell carcinoma, which was human papilloma virus DNA negative (Quest Diagnostics), EBV negative, and p61 positive. $CD4^+$ and $CD8^+$ cells were present in the tumor-containing regions of the biopsy.

In preparation for oncology treatment, he was admitted and underwent a change in cART to a regimen that included tenofovir, emtricitabine, raltegravir, and etravirine, which he received as an inpatient by directly observed therapy. Viral RNA levels promptly declined but did not fall below the limit of detection of 50 copies/mL (Fig. 1). At that time, cisplatin chemotherapy was initiated, and tenofovir was switched to abacavir to avoid potential renal toxicity. He underwent radiation therapy with 70 Gy total delivered to the primary tumor and a comprehensive neck field encompassing levels IA, IB, II, II, and IV. Radiaton therapy was given during an 8-wk course starting 6 September 2012. He received cisplatin 100 mg/m^2 every 3 wk for total of three doses over 6 wk. Repeated measurements of his HIV-1 RNA levels revealed persistently detectable viremia, with slow viral decay, declining to <50 copies/mL with a half-life of ∼6 mo. $CD4^+$ cell numbers declined in response to radiation therapy, as previously reported (21, 22).

The patient did well and had remission in the size of the local lesion. Approximately 6 wk after his last cisplatin therapy, he had recurrence of discomfort in his tongue. In January 2013, he was diagnosed with an overt recurrence of the cancer; CT scans and MRI showed no evidence of local metastatic disease. He underwent radical subtotal glossectomy with reconstructive surgery in March 2013. He tolerated the surgery well and did not have further chemotherapy. He did well, did not require percutaneous endoscopic gastrostomy for feeding, and maintained some speech, which improved after speech therapy. In May–June 2013, there was a local recurrence of the cancer and the development of skin lesions, which gradually increased in size. He initiated do-not-resuscitate status. There were additional symptoms that included difficulty breathing, and he died due to respiratory insufficiency in the emergency room while undergoing evaluation. A limited autopsy showed that he had residual disease at the site of surgery, as well as multiple discrete metastases (skin, larynx, right atrium). Microscopic examination of material from the spleen and several lymph nodes (laryngeal, para-aortic, inguinal, axillary nodes) revealed no histologic or immunohistochemical evidence of squamous cell carcinoma. Local tumor and metastatic lesions showed metastatic invasive squamous cell carcinoma, and all lesions contained lymphoid cells infiltrating the periphery of the tumor. The local tumor contained both $CD4^+$ and $CD8^+$ cells, and metastatic lesions obtained at autopsy contained predominantly $CD4^+$ cells ($CD8^+$ cells were not detected by immunohistochemistry).

The initial description of this patient has been reported (ref. 3, patient 1).

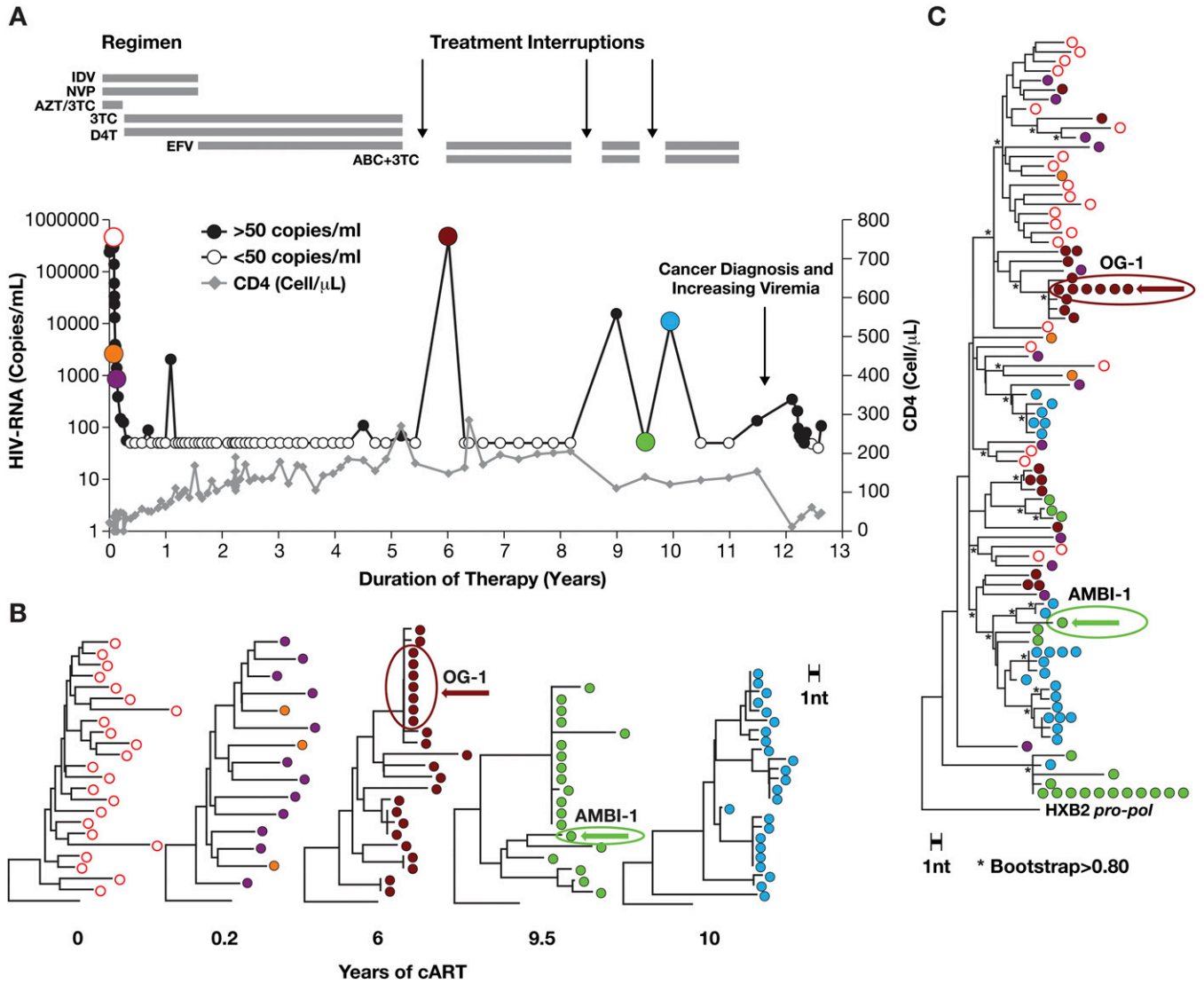

Fig. S1. Clonally expanded cells responsible for low-level viremia emerged from a diverse population of HIV-1–infected cells. (*A*) Time course of HIV-1 viremia (circles) and $CD4^+$ T-cell numbers (gray diamonds) before and following the initiation of combination antiretroviral therapy. (*B*) Plasma samples obtained at the time points indicated by colored circles were subjected to SGS (p6-RT) as described, and neighbor joining phylogenetic analysis was performed. (*C*) Composite neighbor joining tree of all sequences in Fig. S2*B*. *Bootstrap support ≥80% (16).

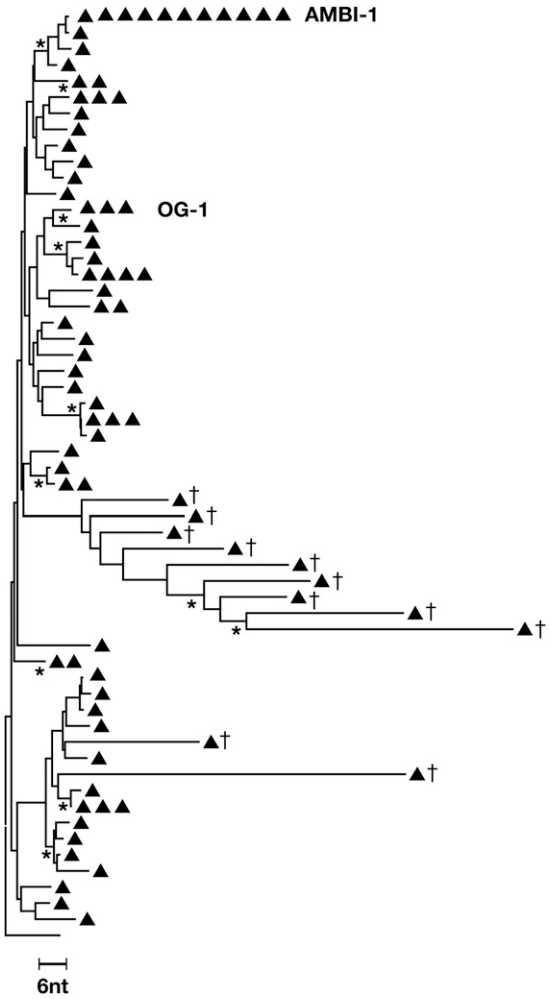

Fig. S2. Cells from the AMBI-1 clone represent a significant fraction of the infected peripheral lymphocytes. PBMCs from the 9 December 2011 (12.1 y after therapy) time point were subjected to SGS (p6-RT) and neighbor-joining phylogenetic analyses were performed. AMBI-1 represented ~13% of the total p6-RT sequences recovered from PBMCs at this time point (there were 83 HIV-1 sequences of which 11 were AMBI-1). Real-time PCR amplification for total HIV-1 DNA (17) revealed that there were 209 HIV-1 DNA copies per 10^6 PBMCs, of which ~13% were AMBI-1, which would correspond to 27×10^6 PBMCs. The peripheral T-cell count was 1,279 cells/μL, and the total number of PBMCs in this patient was estimated to be 3.3×10^{11}, based on total blood volume (Nadler formula) = 5.12 L, assuming that 2% of the total T cells are in the blood. From these estimates, the total number of expanded cells containing AMBI-1 proviruses is calculated to be $\sim 9 \times 10^6$. DNA sequences that correspond to a second clonal virus (OG-1) detected in the ex vivo infectious virus recovery assay were also present. †Hypermutants (5).

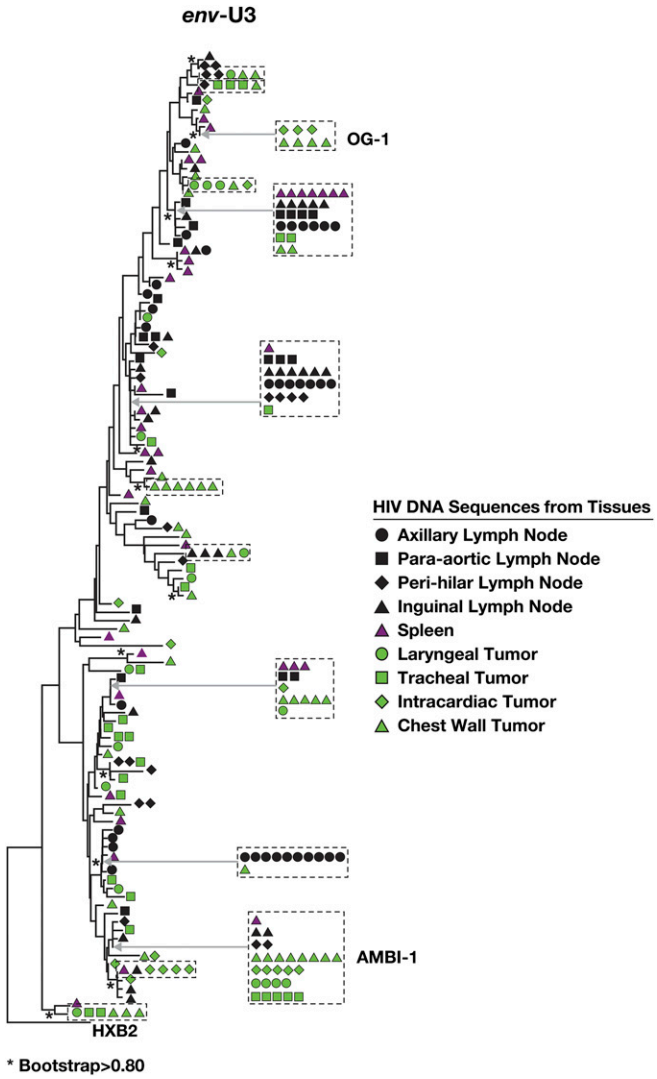

Fig. S3. Phylogenetic analysis of HIV from autopsy tissues. Frozen samples obtained from the indicated autopsy material were subjected to SGS (*env*-U3) and neighbor-joining phylogenetic analysis. For ease of identification, large groups of expanded clones are grouped (boxes), and their position in the tree is noted by arrows.

Table S1. Infection of TZM-bl cells with viral supernatants

Template		2-Fold diluations → Virus dilution in plate									
	A										
No drug	B	1:2	1:4	1:8	1:16	1:32	1:64	1:128	1:256	1:512	Cell control
	C										
	D										
300 nM EFV	E	1:2	1:4	1:8	1:16	1:32	1:64	1:128	1:256	1:512	Cell control
	F										
	G										
	H										
		pNL4-3 Plasmid T1 RLU Minus Cell Control									
		Average	377.62	572.45	692.80	736.23	772.31	566.81	368.27	216.19	108.36
	A										
No drug	B	375.52	530.12	649.92	708.90	721.49	531.50	371.36	201.55	105.19	
	C	363.75	571.90	696.14	747.73	794.75	585.42	389.93	222.46	113.21	
	D	393.58	615.35	732.36	752.07	800.70	583.52	343.51	224.55	106.68	
300 nM EFV	E	−1.09	0.74	0.95	0.83	0.74	0.86	0.66	0.43	0.25	
	F	−1.09	0.04	0.40	0.21	0.02	0.14	0.05	0.04	0.06	
	G	−1.09	−0.16	0.60	0.01	0.01	0.13	0.02	−0.02	0.02	
		Ambiclone T1 RLU Minus Cell Control									
		Average:	36.38	30.34	14.53	6.78	2.78	1.60	0.75	0.23	0.06
	A										
No drug	B	29.97	29.22	15.57	7.29	2.29	1.45	0.57	0.20	0.02	
	C	41.45	31.68	14.52	7.16	3.28	1.33	0.86	0.32	−0.02	
	D	37.71	30.12	13.49	5.89	2.78	2.03	0.83	0.17	0.19	
300 nM EFV	E	−0.30	0.05	−0.05	0.05	−0.01	−0.08	−0.03	−0.08	−0.11	
	F	−0.03	0.20	0.26	0.14	−0.02	−0.04	−0.03	0.06	0.09	
	G	−0.26	−0.01	0.05	−0.02	−0.17	−0.16	−0.14	−0.03	−0.10	
	H										

Infection of TZM-bl cells with serially diluted HEK293T AMBI-1 T1 supernatants was performed as described in *SI Materials and Methods*. Triplicate infections were done with each of the supernatant dilutions in the presence and absence of 300 nm of efavirenz. The data from each infection are shown as relative light units (RLUs) minus the uninfected cell control (sham infection). Virus dilution are color coded: 300 nM Efavirenz (light orange); no drug control (grey). Virus production (average RLU): light green.

Table S2. Summary of biopsy and autopsy tissues

Procedure	Date	Tissue	Type	Anatomic location	Histology	Squamous cell carcinoma markers	Cell equivalents	HIV copies per million cell equivalents	Total SGS	Identical sequences	AMBI-1
Biopsy	7/23/12	Tongue			Squamous cell carcinoma invading tongue	ND	ND	ND	ND	ND	ND
Autopsy	7/2/13	Lymphoid	Spleen		Spleen	p63–	4.4×10^8	37.8	37	19	1
			Lymph node	Peri-hilar	Sinus histiocytosis	p63–	2.4×10^8	161.20	24	12	0
				Axillary	Sinus histiocytosis	p63–	2×10^8	154.00	36	24	0
				Para-aortic	Sinus histiocytosis	p63–	2.5×10^7	21.50	25	20	3
				Inguinal	Sinus histiocytosis	p63–	1.7×10^8	264.30	31	21	2
		Neoplastic	Residual local disease	Laryngeal	Invasive squamous cell carcinoma	p63+	3.3×10^8	18.60	18	12	4
				Tracheal	Invasive squamous cell carcinoma	p63+	9.3×10^6	12.60	27	20	5
			Metastasic lesion	Skin: chest wall	Invasive squamous cell carcinoma	p63+	2.0×10^7	15.80	55	38	7
				Intracardiac	Invasive squamous cell carcinoma	p63+	2.0×10	19.50	22	16	5

Samples were obtained from a biopsy done at the time the tumor was diagnosed, or at autopsy. ND, not done.

Table S3. List of primers used to amplify HIV

Primer set	Primer position	Primer name	Sequence 5′→3′
ENVU3 SGS	Outer	NEF8513FO	GTGCCTCTTCAGCTACCACC
		U39496RO	CTTATATGCAGCTTCTGAGGGC
	Nested	NEF8694FN	GAGGGGACAGATAGGGTTATAGAAG
		U39486RN	TCTGAGGGCTCGCCACTCC
AMBI-1 Provirus	5′ End	UN5140034FO	CATTAGGGCGTGAGCTTGTCTTC
		5264RO	CCTGTATGCAGACCCCAATATG
		UN5140034FN	CTATCAGGGTCAATCCTAGACATTGTG
		5070RN	CACAATCATCACCTGCCATC
	3′ End	4813FO	GTGCAGGGGAAAGAATAGTAGAC
		UN3140034RO	CGTGACAATAAAGAGCTATCTAACCAGAA
		4930FN	TTTGGAAAGGACCAGCAAAGCT
		UN3140034RN	GCACCATCCATAGGGCTTTGTCTTTAG
AMBI-1 RNA	U5-RT	HIVGENF1	CCTTGAGTGCTTCAAGTAGTGTGTGCCCGTCTGT
		3500–	CTATTAAGTATTTTGATGGGTCATAA
		HIVGENF2	AGTAGTGTGTGCCCGTCTGTTGTGTGACTC
		3410–	CAGTTAGTGGTATTACTTCTGTTAGTGCTT
	RT-ENV	3090+	TATCAATACATGGATGATTTGTATGTAG
		6950-	ATGTGTACATTGTACTGTGCTGACAT
		3150+	CTGACTTAGAAATAGGGCAGCATAG
		6850–	GGCACAATAATGTATGGGAATTGG
	ENV-U3	E20F	CAGTTAGTGGTATTACTTCTGTTAGTGCTT
		U39496RO	CTTATATGCAGCTTCTGAGGGC
		E30F	GTGTACCCACAGACCCCAGCCCACAAG
		U39486RN	TCTGAGGGCTCGCCACTCC

Primers used to amplify HIV from DNA and RNA, the *env*-U3 region, and to amplify the full genome of AMBI-1.

Dataset S1. List of integration sites recovered from PBMCs and metastatic tissue

Dataset S1

The AMBI-1 integrant is highlighted.